

# MICROWAVE INSTABILITY SIMULATIONS FOR NSLS-II\*

A. Blednykh<sup>#</sup>, S. Krinsky, B. Nash, Li-Hua Yu  
 BNL, NSLS-II, Upton, New York, 11973-5000, U.S.A.

## Abstract

Potential-well distortion and the microwave instability in the NSLS-II storage ring are investigated. The longitudinal wakepotential is calculated as a sum of the contributions due to vacuum chamber components distributed around the ring. An approximation to the wakepotential for a 0.05-mm charge distribution length, much shorter than the 4.5-mm length of the unperturbed circulating bunch, is used as a pseudo-Green's function for beam dynamics simulations. Comparison of particle tracking simulations using the TRANFT code with the Haissinski solution shows good agreement below the instability threshold current. Above threshold two regimes are observed: (1) energy spread and bunch length are time-dependent (saw tooth behavior); (2) both are time-independent.

## INTRODUCTION

A first estimate of the single-bunch microwave instability threshold was presented in the NSLS-II Conceptual Design Report (CDR) and in the NSLS-II Preliminary Design Report [1,2]. Based on the experience at APS and ESRF, we used a rough approximation of the broad-band longitudinal impedance. Our conclusion was that for a low current bunch length of 4.5 mm (without Landau Cavity), the microwave instability threshold should occur at an average single-bunch current greater than 0.5 mA. This satisfied the baseline requirements for NSLS-II, but it was our belief that this was a very conservative estimate and that the actual threshold would be significantly higher. For a realistic estimate, pseudo-Green's functions for a charge distribution with length  $\bar{\sigma}_s$  much smaller than that of the actual circulating bunch  $\sigma_s$  needs to be computed for the components of the storage ring vacuum vessel. Once the pseudo-Green's function is known, it can be used in a wakepotential tracking code to study the collective behavior. The difficulty is that it requires a great deal of computer time and resources to calculate the wakepotentials for very short charge distributions. In this paper, we discuss the work we have carried out thus far. In the future, we plan to expand our computer cluster and improve our calculations of the pseudo-Green's functions.

## LONGITUDINAL WAKEPOTENTIAL FOR $\bar{\sigma}_s=0.5\text{MM}$ (GDFIDL)

One would like to know the point-particle wakepotential for each component in the ring.

Unfortunately, a method does not exist at the present time to obtain this information. Rather, one must compute the wakepotential using charge distributions of finite length  $\bar{\sigma}_s$  small compared with the bunch length  $\sigma_s$ . To avoid dispersion error, the required computer resources increase rapidly with decreasing driving charge distribution length.

Short-range geometric and resistive-wall longitudinal wakepotentials for  $\bar{\sigma}_s=0.5\text{mm}$  have been computed [3] for the vacuum chamber components and resistive surfaces including: Regular BPMs, User BPMs, Regular Bellows, Scrapers, In-Vacuum Undulators (IVUs), RF cavity transitions, dipole vacuum chambers, multipole vacuum chambers, 717m of Al resistive wall, 30m of stainless steel resistive wall and 45m of Cu resistive wall.

Results for a 3D cavity transition obtained using GdfidL [4] and 2D cavity transition obtained using ABCI [5] agree well for  $\bar{\sigma}_s=3\text{mm}$ . Due to limited computer resources, we have not been able to carry out the GdfidL calculations at  $\bar{\sigma}_s=0.5\text{mm}$  for the cavity transitions so we have used the 2D ABCI code to approximate  $W_{||}(s)$  for a 0.5mm Gaussian bunch.

The IVU [6] is a complex structure and requires large computer resources for its analysis. For this geometry, we are not yet able to compute the wakepotential for a 0.5mm bunch. To proceed, we approximate the complex geometry by an elliptical taper as would be the case for a superconducting undulator (SCU). In order to take into account the fact that the wakepotential for the actual in-vacuum undulators may be larger than for the smooth (SCU) chambers, we have multiplied the SCU results by a factor of 2, which we believe is a conservative estimate.

The total pseudo-Green's function for  $\bar{\sigma}_s=0.5\text{mm}$  is shown in Fig. 1 (blue). The main contributor to the total longitudinal wakepotential is the geometric wakepotential of the IVU transitions which we have approximated by that of 2x15 SCU chambers (green). The resistive wall contribution is also seen to be significant (red).

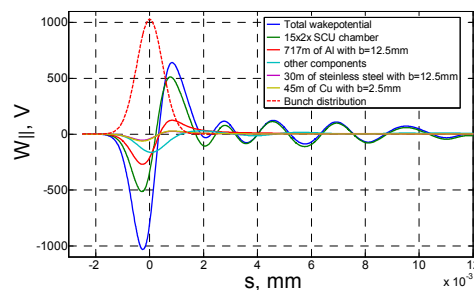


Figure 1: The longitudinal pseudo-Green's function for  $\bar{\sigma}_s=0.5\text{mm}$ . The total wakepotential (blue) will be referred to as the "GdfidL wake."

\*Work supported by DOE contract DE-AC02-98CH10886.

<sup>#</sup>blednykh@bnl.gov

## LONGITUDINAL WAKEPOTENTIAL FOR $\bar{\sigma}_s=0.05\text{MM}$ (ECHO)

For  $\bar{\sigma}_s=0.5$  mm, the tapered transitions for the IVUs were seen to provide the dominant contribution to the longitudinal geometric wakepotential. To estimate the effect of using a pseudo-Green's function corresponding to an even shorter bunch, we approximated the taper cross section by a circular geometry and calculated the short-range wakepotential. This required only modest computer resources. With the help of G. Stupakov, we were able to simulate the short-range wakepotential for a Gaussian charge distribution of 0.05-mm length using the ECHO code [7]. We multiplied the wake computed for the circular taper by a factor of 1.5, since we expect the wake of an elliptical taper to be larger than that for a circular taper. As before, the geometric wake is also multiplied by the additional factor of 2, since the actual wake of an in-vacuum undulator will be larger than that of a smooth elliptical SCU chamber. Resistive wall short-range wakepotentials were calculated separately in mathematica using Piwinski's analytical expression [8] and added to the computed geometric wakepotential. In Figure 2 (right), the blue curve is the wake for  $\bar{\sigma}_s=0.05\text{mm}$  due to 15 circular tapers calculated with ECHO multiplied by  $3=1.5 \times 2$  plus the resistive wall (due to 717m Al, 30m stainless steel and 45m Cu). In Figure 2 (left), the orange curve corresponds to GdfidL wake (from Figure 1) for  $\bar{\sigma}_s=0.5\text{mm}$ . Green curve is the ECHO wakepotential for  $\bar{\sigma}_s=0.05\text{mm}$  [shown in Figure2 (right)] convolved with a 0.5mm Gaussian bunch. We see that the two wakes shown in Figure 2 (left) are quite similar.

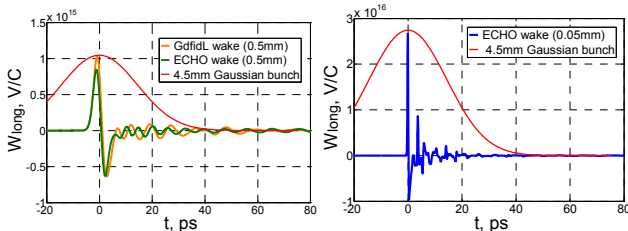


Figure 2: (Left) Orange line corresponds to GdfidL wake (Figure 1) for  $\bar{\sigma}_s=0.5\text{mm}$ . Green line is the ECHO wakepotential computed for  $\bar{\sigma}_s=0.05\text{mm}$  convolved with a 0.5mm Gaussian bunch. Red line is the bunch distribution for a  $\bar{\sigma}_s=4.5\text{mm}$  bunch. (Right) Wake for  $\bar{\sigma}_s=0.05\text{mm}$  due to 15 circular tapers calculated with ECHO multiplied by  $3=1.5 \times 2$  plus the resistive wall (due to 717m Al, 30m stainless steel and 45m Cu).

## MICROWAVE THRESHOLD AND BUNCH LENGTHENING ANALYSIS

The computed longitudinal wakepotentials were applied as input files for the TRANFT particle tracking code [9]. The following parameters for beam dynamic simulations were used: energy  $E=3\text{GeV}$ , momentum compaction

$\alpha_c=0.00037$ , circumference  $C=792\text{m}$ , synchrotron tune  $\nu_s=0.0085$ , Radiation Damping Time  $\tau_e=6.5\text{ms}$ . The energy loss due to synchrotron radiation is compensated in 500MHz RF cavity by longitudinal accelerating field. With damping wigglers in the ring,  $V_{\text{rf}}=3.7\text{MV}$  RF voltage has been specified. The energy spread of the unperturbed (low current) Gaussian bunch is  $\sigma_{\epsilon_0}=9.2 \times 10^{-4}$ . The bunch length is determined by the energy spread, and the low-current bunch duration is  $\sigma_{\tau_0}=15\text{ps}$ .

Two million macroparticles were tracked for 20000 turns (8 damping times). Average values of energy spread and bunch length were calculated as the distribution evolved. In Figure 3, we show the current dependence of the bunch length and the energy spread. We see that although bunch length increases steadily, energy spread shows the threshold behavior characteristic of the microwave instability.

Results of beam dynamics simulations using ECHO wakes for  $\bar{\sigma}_s=0.05\text{mm}$  and  $\bar{\sigma}_s=0.5\text{mm}$  (ECHO wake for  $\bar{\sigma}_s=0.05\text{mm}$  convolved with Gaussian function with  $\bar{\sigma}_s=0.5\text{mm}$ ) shown in Figure 3, demonstrate that the behavior of the microwave threshold current is sensitively dependent on the charge distribution length  $\bar{\sigma}_s$  used to calculate the pseudo-Green's function. The threshold current is  $\sim 50\text{mA}$  for  $\bar{\sigma}_s=0.5\text{mm}$  (green line) and  $\sim 5\text{mA}$  for  $\bar{\sigma}_s=0.05\text{mm}$  (blue line). Therefore, to accurately determine the microwave instability threshold, it may be necessary to compute the pseudo-Green's function for  $\bar{\sigma}_s \approx \sigma_{s0} / 100$ , where  $\sigma_{s0}$  is the unperturbed (low-current) length of the bunch stored in the ring.

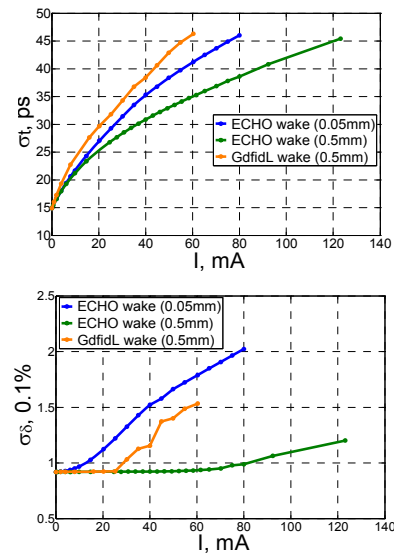


Figure 3: (Top) Bunch lengthening as a function of current for: ECHO wake ( $\bar{\sigma}_s=0.05\text{mm}$ , blue); ECHO wake ( $\bar{\sigma}_s=0.5\text{mm}$ , green); GdfidL wake ( $\bar{\sigma}_s=0.5\text{mm}$ , orange). (Bottom) Energy spread as a function of current: ECHO wake ( $\bar{\sigma}_s=0.05\text{mm}$ , blue); ECHO wake ( $\bar{\sigma}_s=0.5\text{mm}$ , green); GdfidL wake ( $\bar{\sigma}_s=0.5\text{mm}$ , orange).

The two wakepotentials shown in Figure 2 (left) (GdfidL and ECHO) for  $\bar{\sigma}_s=0.5\text{mm}$  have similar short-range part ( $t \leq 10\text{ps}$ ), but the instability thresholds are significantly different. This indicates that the longer range oscillating tails play a non-negligible role. We plan to investigate this further. We have increased the size of our computer cluster and plan to compute the more realistic 3D wakepotentials using GdfidL for  $\bar{\sigma}_s$  down to 0.05mm for the components distributed around the ring.

In Figure 4, we plot the dependence of the rms energy spread on the number of revolutions around the ring due to the effect of the ECHO wakepotential for  $\bar{\sigma}_s=0.05\text{mm}$  [Fig. 2 (right)]. From Figure 4, we see that below 20mA, the energy spread approaches equilibrium. Above this current level there is more complicated time-dependent behavior, including saw tooth type instability.

At still higher currents the energy spread again becomes time-independent. This reminds one of the type of behavior observed in the SLAC damping ring [10].

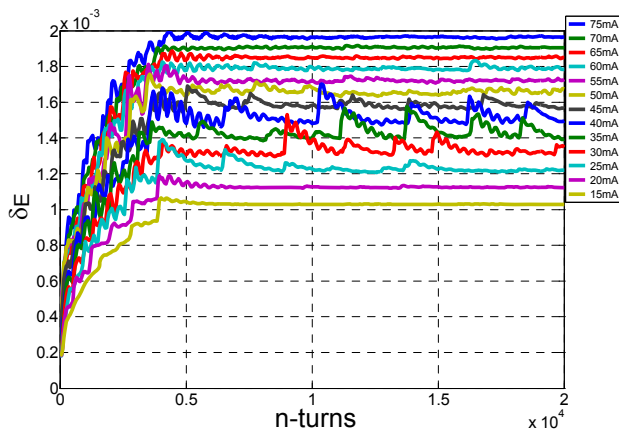


Figure 4: The turn-by-turn rms energy spread for different values of current using ECHO wakepotential with  $\bar{\sigma}_s=0.05\text{mm}$  in TRANFT simulation code.

### COMPARISON WITH HAISSINSKI EQUATION [11]

To model the potential-well distortion effects, the GdfidL wake for  $\bar{\sigma}_s=0.5\text{mm}$  (Figure 2, left, orange) was used in a Haissinski equation solver (written in Mathematica) and in the particle tracking code TRANFT. Below threshold, simulation results were found to give equilibrium bunch distributions in good agreement with the Haissinski equation, as can be seen from the results shown in Figure 5.

### CONCLUSION

The calculations reported in this note suggest that the microwave threshold will occur at an average single bunch current greater than 5 mA. In the future, we hope to

obtain better approximations for the wakes and thus obtain more accurate approximations for the microwave threshold.

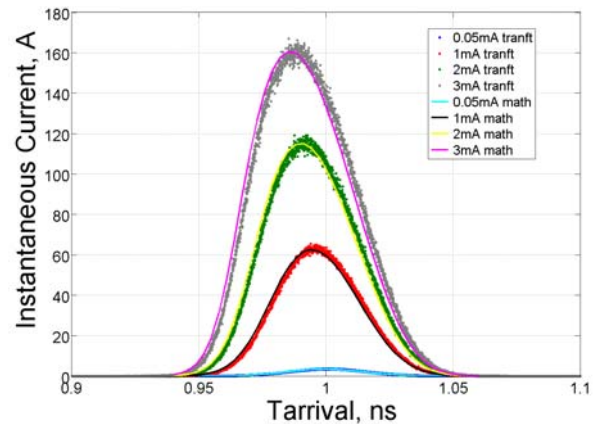


Figure 5: Bunch profiles for different current values using GdfidL wakepotential for  $\bar{\sigma}_s=0.5\text{mm}$  shown in Fig. 2 (left). Dots correspond to particle tracking simulations and smooth curves correspond to Haissinski solution. The four curves correspond to average bunch currents of 0.05mA, 1mA, 2mA and 3mA.

### ACKNOWLEDGEMENTS

We wish to thank K. Bane and G. Stupakov for sharing their expertise on the microwave instability with us during very stimulating visits to NSLS-II. We also thank M. Blaskiewicz for providing TRANFT and for guidance in setting up and running the code.

### REFERENCES

- [1] NSLS-II Conceptual Design Report, 2006; <http://www.bnl.gov/nsls2/project/CDR/>.
- [2] NSLS-II Preliminary Design Report, 2008; <http://www.bnl.gov/nsls2/project/PDR/>.
- [3] A. Blednykh, „Impedance Calculations for the NSLS-II Storage Ring”, Tech Note, 2008.
- [4] W. Bruns, GdfidL code; <http://www.gdfidl.de>.
- [5] Y. H. Chin, ABCI code.
- [6] A. Blednykh and et al., “Transverse Impedance of Small-Gap Undulators”, EPAC06, 2970.
- [7] I. Zagorodnov, ECHO code.
- [8] A. Piwinski, DESY Report 72/72, 1972.
- [9] M. Blaskiewicz, “The TRANFT User’s Manual version 1.0”, BNL-77074-2006-IR, 2006.
- [10] B. Podobedov, PhD Thesis, SLAC-R-543, 1999.
- [11] J. Haissinski, Il Nuovo Cimento 18, 72, 1973.